

Received August 11, 2019, accepted August 19, 2019, date of publication August 22, 2019, date of current version September 16, 2019.

Digital Object Identifier 10.1109/ACCESS.2019.2936822

RUL Prediction of Lithium-Ion Battery Based on Improved DGWO-ELM Method in a Random Discharge Rates Environment

JUN ZHU^{ID}, TIANXIONG TAN, LIFENG WU^{ID}, (Member, IEEE),

AND HUIMEI YUAN^{ID}, (Member, IEEE)

College of Information Engineering, Capital Normal University, Beijing 100048, China

Beijing Key Laboratory of Electronic System Reliability Technology, Capital Normal University, Beijing 100048, China

Corresponding author: Huimei Yuan (4394@cnu.edu.cn)

This work was supported in part by the National Natural Science Foundation of China under Grant 61873175, in part by the Key Project B Class of Beijing Natural Science Fund under Grant KZ201710028028, in part by the Capacity Building for Sci-Tech Innovation-Fundamental Scientific Research Funds under Grant 025185305000-187, in part by the Youth Innovative Research Team of Capital Normal University, and in part by the Beijing Youth Talent Support Program under Grant CIT&TCD201804036.

ABSTRACT Lithium-ion batteries are widely applied in many fields. It is important for predicting battery life (RUL). It is randomly discharged that the lithium-ion battery under random conditions. The experiment of constant current discharge cannot simulate the discharge state under working conditions. Based on the data collection of the NASA dataset, the DGWO-ELM algorithm is proposed to predict lithium-ion battery. The DGWO-ELM is composed of Extreme Learning Machine (ELM), Grey Wolf Optimization (GWO), and Differential Evolution (DE) for the purpose of improving the accuracy of prediction. The algorithm uses GWO algorithm to optimize the weight and threshold of ELM and improves the three deficiencies in the GWO algorithm. The DGWO-ELM algorithm is proved preferably than ELM predictor improved by particle swarm optimization (PSO-ELM) and SVM predictor improved by Grey Wolf Optimization (GWO-SVM). The algorithm is verified by NASA's lithium-ion battery constant current discharge data, and then used to predict the RUL of the lithium-ion battery in a random discharge environment. The results show that the DGWO-ELM performs well on improving the accuracy of prediction.

INDEX TERMS Lithium-ion batteries, RUL, random discharge, DGWO, DE, ELM.

NOMENCLATURE

a, b, c	a mutated individual	MC_m	the DE algorithm mutated to get population
b	the hidden layer offset	Met_m	the intermediate population
b_{\max}	the upper bound of scaling factor	m_val	the mutation target value
b_{\min}	the lower bound of scaling factor	p_val	the parent target value
CP	the crossover probability	R	the training period
c_val	the filial generation target value	R^2	the R-Square
d	the process parameters.	W	the randomly generate weights
D_k	the adaptive factor	$X_\alpha, X_\beta, X_\gamma$	the location update
$D_\alpha, D_\beta, D_\gamma$	a stochastic process	α, β, γ	the three best target values
H	the output matrix of the hidden layer	δ	the scaling factor
K	determined by the action radius of the current position and the action radius of the previous position		
$MAE, RMSE$	the mean absolute error and root mean squared error		

The associate editor coordinating the review of this article and approving it for publication was Qiquan Qiao.

ABBREVIATIONS

BMS	Battery Management System
DE	Differential Evolution
ELM	Extreme Learning Machine
GWO	Grey Wolf Optimization

PSO	Particle Swarm Optimization
RUL	Remaining useful life
SVM	Support Vector Machine

I. INTRODUCTION

Today, lithium-ion batteries are very popular in electronics industry with numbers of advantages such as high-energy density, high open-circuit voltage and output power, and wide range of operating temperature. The highlight function is that lithium-ion batteries can be charged and discharged at any time although they are not running out of power. Therefore, many types of electronic products benefit from lithium-ion batteries. For example, in recent years, lithium-ion batteries have been applied in most energy vehicles as their power source. More and more people choose to use energy vehicles which could contribute to protect natural environment. Endurance and safety are the major concern in the selection of energy vehicles. Because people are getting used to focus on the life and safety of lithium-ion batteries. The remaining useful life of batteries is defined by the number of charging and discharging circles and the lifespan of batteries. The chemical substances in batteries will age by the increase of working time, which could cause a number of severe problems when aging to a certain extent [1]. Therefore, the battery aging issues, such as the explosion of Samsung Note7 and the recall of spontaneous combustion of Tesla Model S, all emphasize the importance of lithium-ion battery safety.

The aging degree of battery cannot be directly measured. However, the rest of battery's life time could be predicted, which could be the measurement of the aging degree of battery. There are two RUL prediction methods for lithium-ion batteries, which are model-driven and data-driven methods [2]. The core of the model-driven methods is to approximate the Probability Density Function (PDF) of systematic random variables with some discrete and random sampling points. Guo et al. have analyzed some recent methods of dual Kalman filters (KF) algorithm and found that it is necessary for the State-Of-Charge (SOC) battery prediction to use multi-scale parameter adaptive method [3]. Chen et al. have claimed another method, which combines the model adaptive, noise adaptive and UKF algorithm to predict the RUL [4]. However, this method relies too much on the particle number, quality of historical data [5]. Luo et al. have used KF based on cubature Kalman filter (CKF) to predict the SOC [6]. The model-driven method also includes [2], [5], [7]–[11]. It is important for the model-driven methods to require an accurate reference model and appropriate parameter settings. Otherwise, the accuracy of prediction algorithm cannot be further improved.

Data-driven methods include evolutionary algorithm, machine learning algorithm, neural network algorithm, etc. Wang et al. have used the expectation–maximization (EM) algorithm and the first hitting time (FHT) method in probability perspective to predict the RUL [12]. Deng et al. have proposed the estimation method of Least Squares Support Vector Machine (LSSVM) to establish the State-Of-Health (SOH)

model to make the battery model suitable for multiple working conditions and to calculate the RUL of the battery at the end of life [13]. Li et al. proposed the improved bird swarm algorithm optimization least squares support vector machine (IBSA-LSSVM) model to predict the remaining life of lithium-ion batteries [14]. Li et al. have used Stacked Denoising Autoencoders-Extreme Learning Machine (SDAE-ELM) algorithm based on a big data driven method to predict the RUL [15]. Yang et al. [16], [17] firstly claimed the Improved Extreme Learning Machine (IELM) based on the combination of Extreme Learning Machine and used HKA-ELM algorithm based on Heuristic Kalman Algorithm (HKA) and ELM to predict the RUL of Lithium-ion batteries by remaining the particle diversity. Zhao et al. have employed long short-term memory based on a data-driven model to estimate the RUL [38]. The data-driven method also includes [18]–[21]. Although these battery prediction methods have high RUL prediction accuracy at a constant discharge rates, these prediction methods do not consider the effect of discharge rate and other factors.

The capacity of the lithium-ion battery is closely related to ambient temperature, relaxation effect, self-heating, and the discharge rate of the battery. The relaxation effect could lead to the recovery of the battery, increases the available capacity for the next cycle [27]. Over-discharged cell also accelerates the aging rate under a normal cycle [35]. Amine et al. found that the capacity fade increases from 40% to 70% as the temperature increases from 37 °C to 55 °C [34], [35]. Bryden et al. found that the cells discharged at 1 C and 3 C have increased by 34.7 % and 57.4 % respectively [28]. Meng et al. found that the maximum temperature is 58.88 °C and 42.33 °C at the end of 2 C and 1 C discharge rate [29], [30]. When a discharge rate is changed from a high rate to a low rate, most ‘lost’ capacity caused by the high rate is revoked [31]. The higher a discharge rate, the smaller a usable capacity. Therefore, an important issue is that the RUL can be predicted in a random discharge rates environment, which is very important for the scholars. In practical applications, it is inevitable that the discharge current of lithium-ion batteries could change. Researchers began to study the RUL prediction of batteries under the random discharge circumstance. The discharge current, and temperature of lithium-ion batteries used for electric vehicles (EVs) change dramatically under the working conditions. Zhang et al. used the Box-Cox transformation (BCT) and Monte Carlo (MC) simulation to predict RUL [32]. Improving battery voltage prediction in an electric bicycle used altitude measurements and kernel adaptive filters under the working conditions [20]. Liu et al. proposed a SOC of deep-discharging lithium -ion batteries estimation method using a novel partial adaptive forgetting factors recursive least square (PAFFRLS) under complicated working conditions at different temperatures [33]. Wang et al. designed an experiment including the battery capacity reduction with different discharge rates under four cycles and predicted the RUL of battery at different discharge rates [22]. However, in the experimental discharge cycle, only four discharge rates

are changed. It is obvious that this experimental design is too simple to explain the concept of random discharge and still needs to be improved. Wu et al. have used Gamma function model to predict the RUL of lithium-ion batteries based on the randomized battery usage dataset published by NASA [23]. However, because the randomized battery usage dataset is too linear, and the article does not compare with other data to verify the quality of the model, the experimental results are still unpersuasive.

Lithium-ion batteries are affected by many factors under working conditions, and the capacity fade curves of different specifications are also different. Using model-driven method difficult describe the RUL of lithium-ion battery of different specifications under complex working conditions [39]. Therefore, this paper uses a data-driven method to solve the above problem.

The Grey Wolf Optimizer (GWO) algorithm is a new heuristic algorithm. The advantages of the algorithm are that it has excellent ability to find the optimal solution and parameter is easy to set and implement [24]. So the algorithm has been widely used in the field of scientific research. Compared with the Particle Swarm Optimization (PSO) algorithm [25], the GWO algorithm is memoryless and changes the size of the population by elimination. It can also control the entire population to move to the optimal region at a constant speed. The PSO algorithm controls individual movement through individual information sharing. So it is obvious that PSO algorithm is faster to converge to the optimal solution. But it is also easier to trap in local optimum. Each wolf group of the GWO algorithm is generated by the original wolves, which means that the accuracy of the GWO algorithm is largely determined by the selected leader of wolf. If the selection of the leader wolf fails, the algorithm will converge in advance and the accuracy will be lower. When all the individuals in the middle and late stages approach the prey, this algorithm is easily running into the local optimization solution, resulting in lack of diversity of algorithms. Then the algorithm combines another evolutionary algorithm, Differential Evolution Algorithm, to strengthen the robustness of the wolves to prevent the GWO from falling into the local optimal solution.

When the kernel function is determined, the mapping mode of Support Vector Machine (SVM) algorithm becomes unique [13]. So when mapping to a high-dimensional space, there is only one or a few chances to choose a model. If a good model is not selected, it will not only make the algorithm worse, but also slow down the training speed of the SVM algorithm. Then the algorithm combines ELM algorithm [15]. Compared with the SVM algorithm, the ELM algorithm has various ways for mapping to high-dimensional space, which can make solution for the single mapping mode of SVM algorithm and increase the probability of randomization to fit the model to solve SVM algorithm training speed.

ELM algorithm mapping problem to a high-dimensional space, by the way of passive mapping to generate a random input weights and thresholds. Although there is a fast training speed, the prediction result is affected by random mapping.

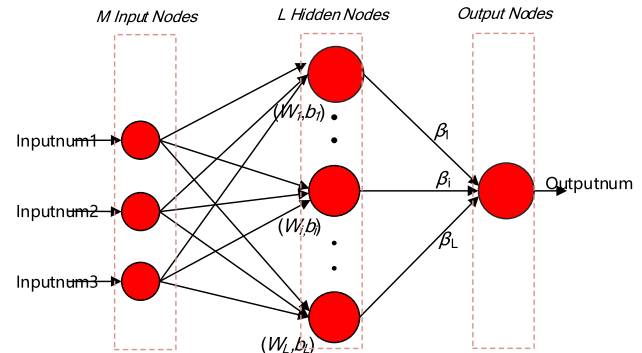


FIGURE 1. Principle of ELM.

Therefore, this paper uses the GWO algorithm to optimize the input weights and thresholds after the randomization of the ELM algorithm.

There are three important improvements for the original GWO algorithm. Firstly, it needs to change the search mode to the mode of lithium-ion battery degradation. The second part is to add the gray wolf group system of hierarchy to the wolves. The wolf rank parameter is determined and updated by the GWO algorithm. The third improvement is to add memory factors to strengthen the relationship between individuals and populations in the algorithm, making it easier for the algorithm to reach the optimal solution.

In this experiment, it considers the uncertainty of random discharge of lithium-ion batteries under working conditions to predicts the RUL. This experiment discards the conventional constant current discharge battery dataset and uses the randomized battery usage dataset published by NASA. This experiment improves the three deficiencies in the GWO algorithm. The improved GWO algorithm is combined with ELM algorithm and DE algorithm to obtain the DGWO-ELM algorithm. The DGWO-ELM is compared with GWO-SVM and PSO-ELM algorithm to verify the effectiveness of the algorithm. The algorithm improves the defects in the respective algorithms and has good effect on prediction.

In this paper, section two introduces theories of ELM, GWO, DE and DGWO. Section three shows experiments and results. Section four analyzes experimental results and compares GWO-SVM algorithm and PSO-ELM algorithm with other improved algorithms. Section five gives our conclusion and expectation.

II. DGWO-ELM ALGORITHM

A. ELM ALGORITHM

The ELM algorithm consists of three layers: the input layer, the hidden layer and the output layer. The weights and biases are randomly selected in this neural network. Then the output weights are determined according to the least-squares method [16]. Figure 1 shows the process of ELM algorithm.

Where L is the number of hidden layer nodes. Weight W are randomly generated between the input layer and the hidden layer. The hidden layer offset is set as b , and activation

function is expressed by $G(x)$. Calculating the output matrix of the hidden layer get H .

$$W = \begin{pmatrix} w_{11} & \cdots & w_{1m} \\ \vdots & \ddots & \vdots \\ w_{i1} & \cdots & w_{im} \end{pmatrix}_{i \times m} \quad (1)$$

$$b = \begin{pmatrix} b_1 \\ \vdots \\ b_i \end{pmatrix}_{i \times 1} \quad (2)$$

$$H = \begin{pmatrix} G(w_1, b_1, x_1) & \cdots & G(w_l, b_l, x_1) \\ \vdots & \ddots & \vdots \\ G(w_1, b_1, x_n) & \cdots & G(w_l, b_l, x_n) \end{pmatrix}_{n \times l} \quad (3)$$

Using generalized inverse matrix of hidden layer calculate output weights β .

$$\sum_{i=1}^l \beta_i G(w_i, b_i, x_j) = t_j, \quad j = 1, 2, \dots, m \quad (4)$$

$$H\beta = T \quad (5)$$

$$\beta = H^+T \quad (6)$$

B. DGWO-ELM ALGORITHM

Because the input weights and bias of ELM are randomly generated, which will affect the prediction results. This paper uses the GWO algorithm to optimize the prediction framework of ELM. And then this experiment improves three deficiencies in the GWO algorithm according to the laws of cell deterioration. The improved GWO algorithm is combined with DE algorithm in order to prevent falling into local optimum. The DGWO algorithm combine with ELM algorithm to obtain the DGWO-ELM algorithm. Figure 2 shows the process of DGWO-ELM algorithm.

Initialization parameter: where n is population size, N_{iter} is iterative times, b_{max} is upper bound of scaling factor, b_{min} is lower bound of scaling factor, CP is crossover probability, $popnum$ is variable dimension, $input_{train}$ is input matrix, and $output_{train}$ is output matrix.

Data normalization: the input matrix and output matrix is normalized to get $input_{train1}$, $output_{train1}$.

Population initialization: the spatial target of the GWO algorithm is initialized to get p . Substituting p , $inputnum$, $Hiddenum$, $input_{train1}$, $output_{train1}$ into the ELM algorithm calculate the parent target value p_val . This process is repeated to get the filial generation target value c_val and the mutation target value m_val .

The improved GWO algorithm determine the rank of the parental population. The closer the target value of the parental population get to the target distance, the higher rank of the population. The three best target values are set to α , β , γ in the parent population, respectively. The values of α , β , γ are expressed as $parent_1$, $parent_2$, $parent_3$.

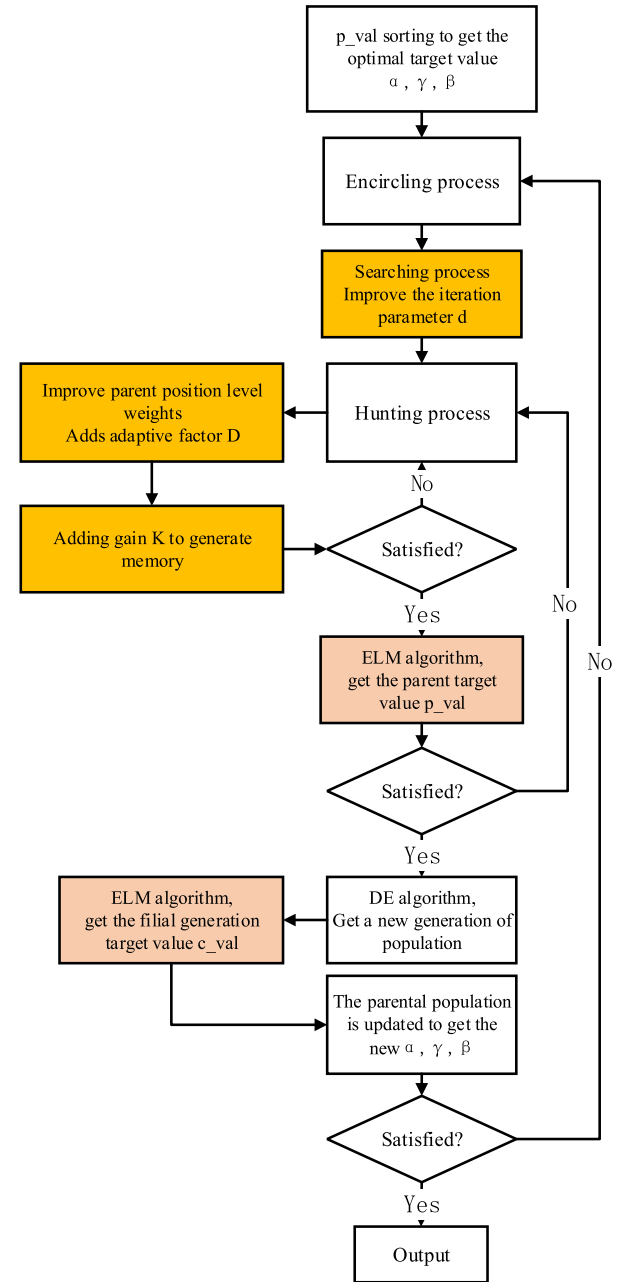
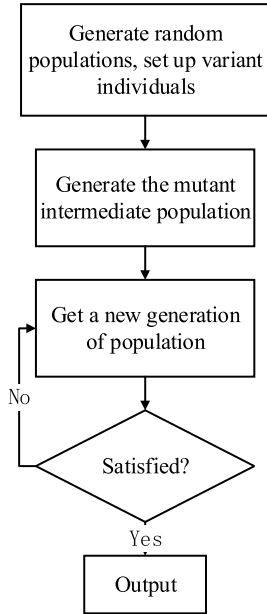


FIGURE 2. Principle of DGWO-ELM.

Where d , $rand1$, $rand2$ is the process parameters, which are random values between -1 and 1 .

$$d = 2 - 2 \frac{N_{iter}^i}{N_{iter}}; \quad d \in [0, 2] \quad (7)$$

In the process of searching for prey, the wolf group always approach the target at a constant step-size. For the lithium-ion battery data, the increase of the period making the capacity fading of the lithium-ion battery faster, and the convergence speed of the algorithm is affected, which will affect the experimental results. According to the above shortcomings, this paper changes the exploration model to an index model,

**FIGURE 3.** Principle of DE.

which adds convergence factor to control the early convergence speed, to adapt the various capacity data (variable current data and non-variable current data). Model is as follows:

$$d = w * \left(1 - \exp\left(1 - \frac{N_{iter}^i}{N_{iter}}\right)\right); \quad d \in [0, 2] \quad (8)$$

Hunting process: where D_α is the action radius of α , X_α is the location update of α . The formula 11 and 12 are repeated to obtain the action radius D_β , D_γ and the location update X_β , X_γ . According to the location update X_α , X_β , X_γ , the location X is obtained.

$$A_\alpha = 2 * d * rand1 - d \quad (9)$$

$$C_\alpha = 2 * rand2 \quad (10)$$

$$D_\alpha = |C_\alpha * parent_1(t) - parent_{pr}(t)| \quad (11)$$

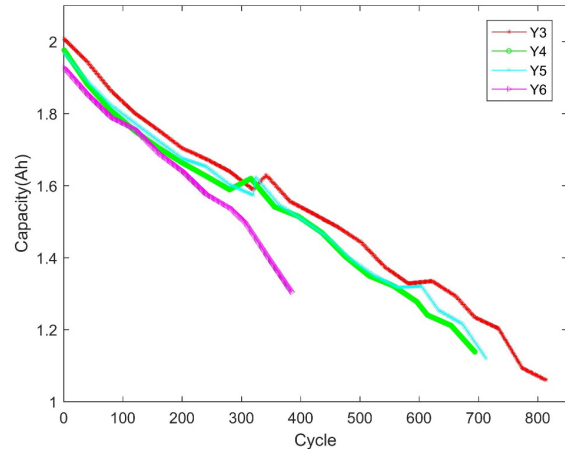
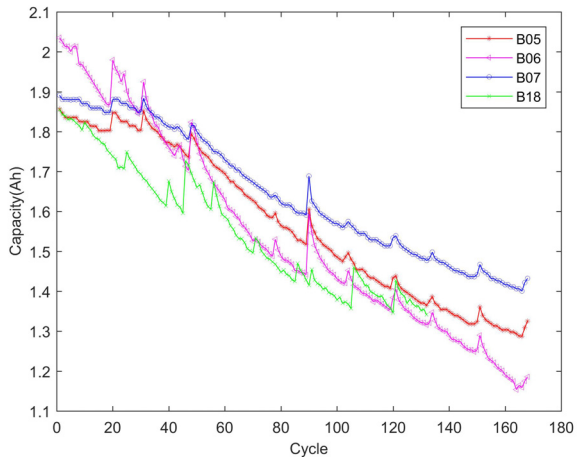
$$X_\alpha = parent_1(vr) - A_\alpha^* D_\alpha \quad (12)$$

$$X = \frac{X_\alpha + X_\beta + X_\gamma}{3} \quad (13)$$

The traditional GWO algorithm does not set weight in formula 13, which count the X_α , X_β , X_γ as the same rank. In order to reflect the rank of the wolves, the adaptive factor D_k is added to the improved algorithm, and the other adaptive factor D_z is determined by the action radius of the three positions.

The traditional GWO algorithm is memoryless. Referring to the gain and state equation of the Kalman algorithm, the algorithm introduces the parameter K and the state update equation. Where K is determined by the action radius of the current position and the action radius of the previous position. The improved formula is 14.

$$D_z = D_\alpha + D_\beta + D_\gamma \quad (14)$$

**FIGURE 4.** Change in capacity of batteries Y3, Y4, Y5, Y6 under randomly varied discharge.**FIGURE 5.** Change in capacity of batteries B05, B06, B07, B18 under constant current discharge cycle.

$$K = 1 - \frac{D_\alpha(t-1)}{D_\alpha(t)} \quad (15)$$

$$X(t) = \frac{1}{D_z} * \left(\sum_{k=\alpha, \beta, \gamma} D_k^* X_k \right) + K^* v \quad (16)$$

$$v = \rho^*(parent_1(t) - parent_{pr}(t)) \quad (17)$$

where $[min c, max c]$ is the variable value range to prevent the X out of bound.

$$parent_{pr}(t) = X, X \in [min c, max c] \quad (18)$$

When it finish iteration, position vector $parent_{pr}$ of all the population are brought into ELM algorithm to get the parent target value p_val . And then deciding whether it get all the best parent goal values.

DE algorithm mutate to get population Met_m , a, b, c is mutated individual, δ is scaling factor.

$$MC_m = parent_m(a) + \delta * (parent_m(b) - parent_m(c)) \quad (19)$$

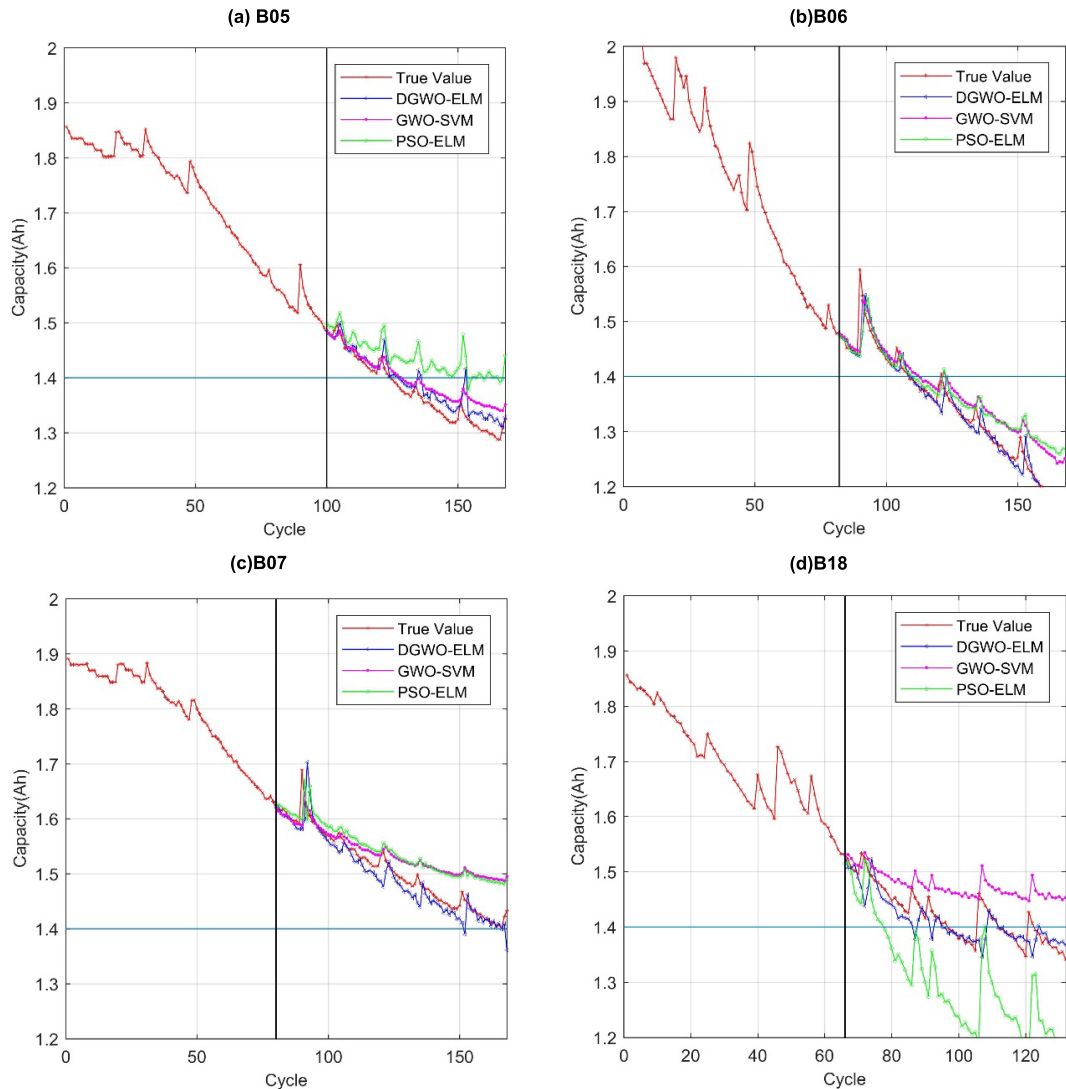


FIGURE 6. RUL prediction results for three algorithms to B05, B06, B07, B18 under constant current discharge cycle.

Variable is set scope to prevent population from crossing the boundary, to get the intermediate population Met_m .

$$Met_m = MC_m, MC_m \in [\min c, \max c] \quad (20)$$

Parental population and intermediate population perform cross operation which exchange the dimension $j[1, 2, 3, \dots, D]$, when the random probability is less than the crossover probability. Individuals are selected from the original and intermediate population to obtain a new generation of population.

$$z = \begin{cases} parent_{ch}, & ch = j, rand < CP \\ Met_{ch}, & ch \neq j, rand \geq CP \end{cases} \quad (21)$$

New population is substituted into ELM algorithm to obtain filial generation target value c_val . The DE algorithm process is repeated to get all the filial generation population. After comparing the filial generation target value with the parent

target value, if the filial generation target value is better than the parent target value, the filial generation target value replaces the parent target value and vice versa. Update the α, β, γ . After completing the iteration, the algorithm uses regression to predict results.

III. EXPERIMENT AND RESULTS

A. NASA DATA SET

In this essay, the RUL prediction with DGWO-ELM algorithm is based on the experiment data of the NASA battery group. These data used the data set of the random discharge experiment published by NASA. Battery 03, 04, 05 and 06 are selected as the experiment data which have the same type, brand and the difference only in volume degradation rate. The test temperature for this experiment was set constantly at 25 °C (regardless of battery self-heating). During the discharging process, the discharge current changes randomly

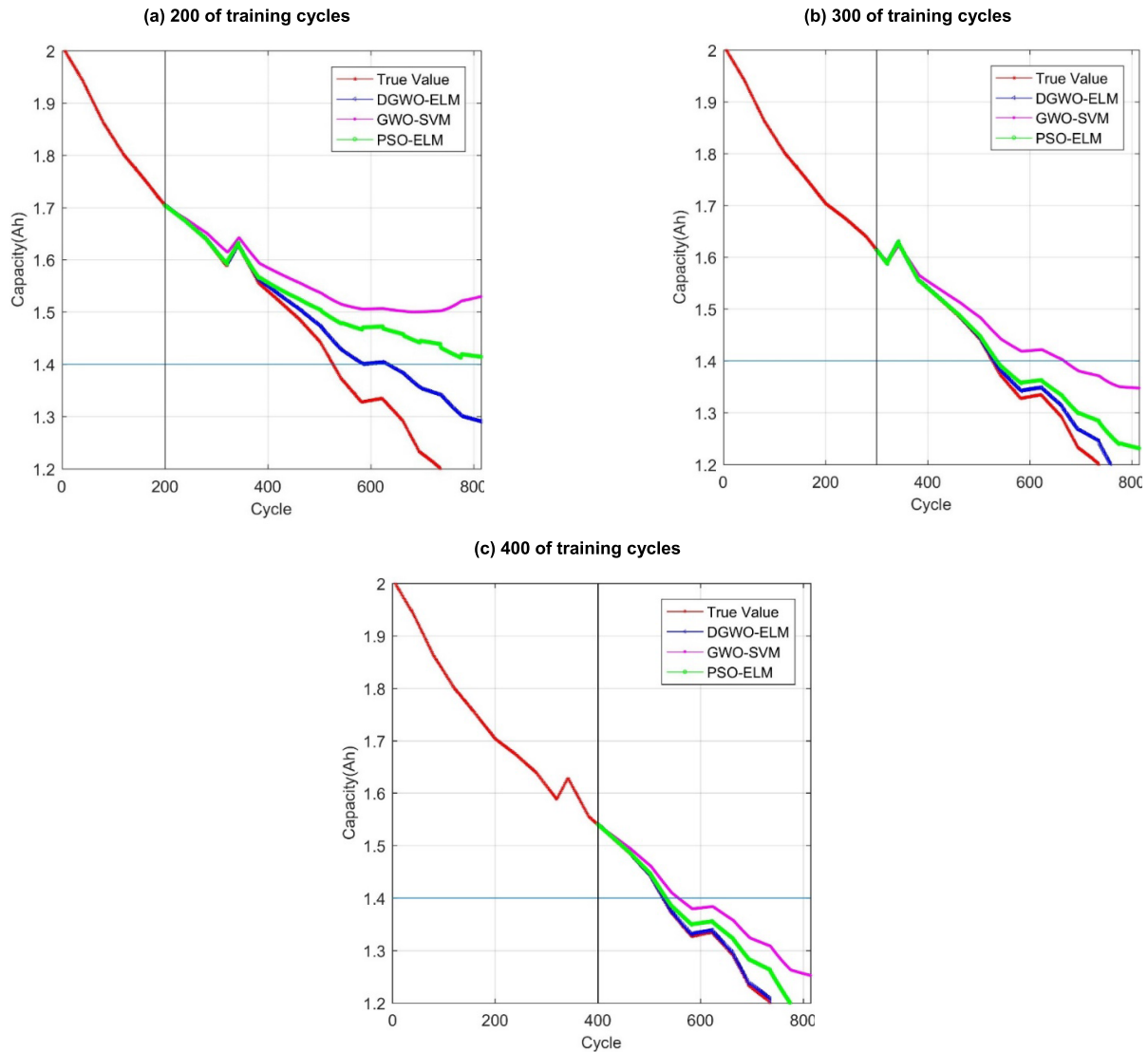


FIGURE 7. Three algorithm prediction results of Y3 dataset under randomly varied discharge.

every 5 minutes in each discharging cycle (The size of the change is undetermined) until the set voltage reaches the threshold. During the charging process, the battery is charged with a constant current of 1C until the threshold is reached. The charging and discharging process are repeated until the battery failure. In the random current discharge experiment, the battery capacity is represented by only 10 to 20 data due to the amount of monitoring points set by NASA. Therefore, this experiment linearizes the data. Figure 4 is the chart of the changes in capacity of the battery Y3, Y4, Y5 and Y6 under randomly varied discharge cycles.

The experimental data of random discharge rate is too linear and may not fully explain the effectiveness of the algorithm. So this experiment uses NASA's constant current discharge experimental data to verify the algorithm. Battery 05, 06, 07 and 18 are selected.

B. RESULTS

The failure threshold of the battery is set to 1.4Ah in this paper. Figure 5 is the chart of RUL prediction results for three algorithms to B05, B06, B07, B18.

B05, B06, B07, B18 data are trained respectively for 100, 80, 80, 66 cycles. In Figure 6, red curve represents the output true value. Blue curve represents the prediction results of DGWO-ELM. Purple curve represents the prediction results of GWO-SVM. Green curve represents the prediction results of PSO-ELM. Black vertical line represents the length of the training cycle. Light blue line represents the battery capacity failure threshold. It can be clearly seen from Fig. 6 that the prediction results of the DGWO-ELM algorithm represented by the blue line is always the best, regardless of the different training data or different training cycles. In some data sets, the PSO-ELM algorithm has good

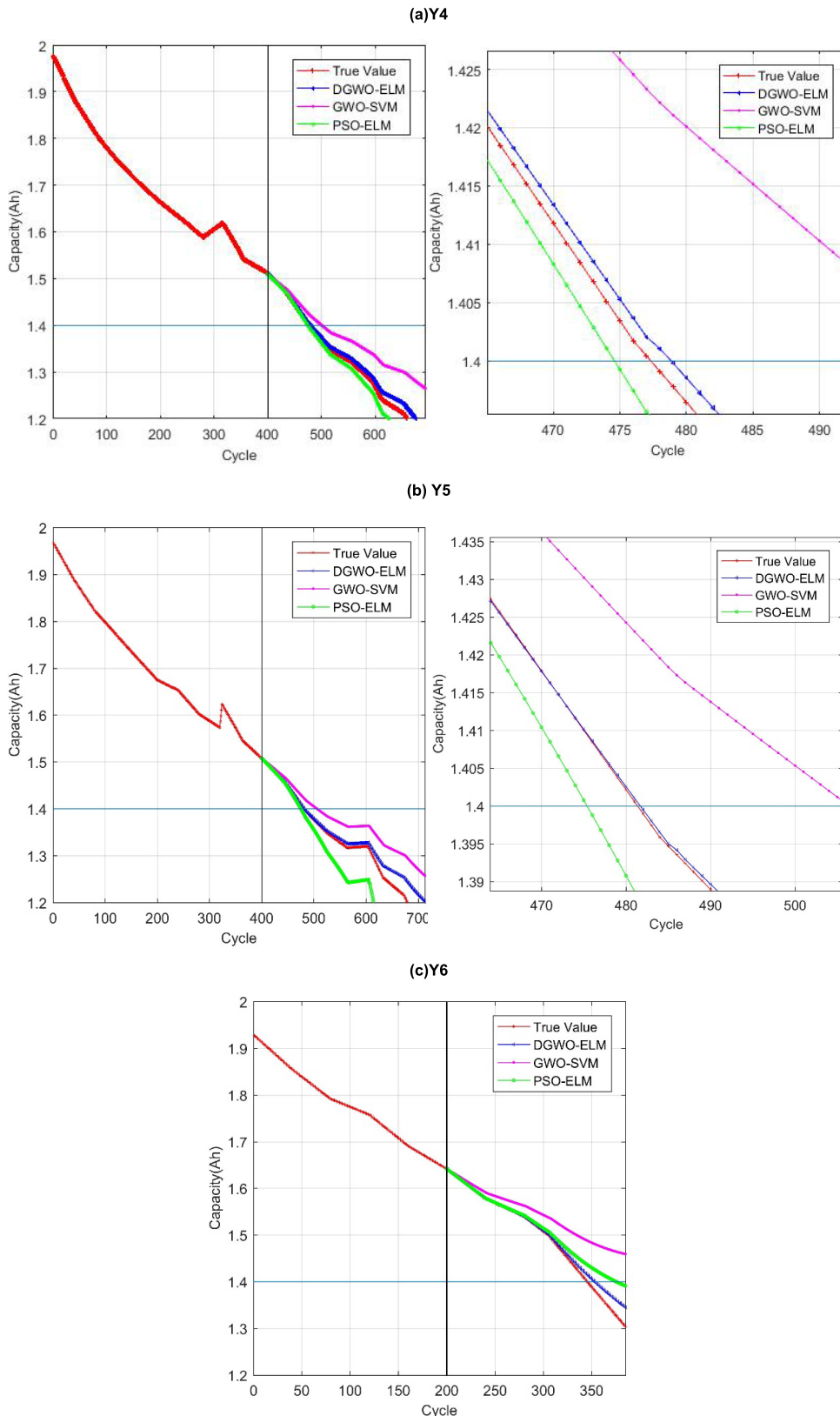


FIGURE 8. RUL prediction results for three algorithms to Y4, Y5, Y6 under randomly varied discharge.

prediction results, and the worst prediction algorithm is the GWO-SVM.

The experiment using the same data, compares the DGWO-ELM algorithm with GWO-SVM and PSO-ELM,

TABLE 1. Comparison of two algorithm results under different data sets and cycles of random discharge.

Battery	Algorithm	R(cycle)	MAE	R^2	RMSE
Y3	DGWO-ELM	200	0.0015169	0.99962	0.0023059
	PSO-ELM	200	0.0042781	0.99775	0.0052340
	DGWO-ELM	400	0.0019154	0.99959	0.0017695
	PSO-ELM	400	0.0025723	0.99892	0.0034932
Y4	DGWO-ELM	150	0.0022390	0.99828	0.003197
	PSO-ELM	150	0.0107966	0.99187	0.009275
	DGWO-ELM	400	0.0004357	0.99997	0.0005068
	PSO-ELM	400	0.0006032	0.99995	0.0006368
Y5	DGWO-ELM	150	0.0021834	0.99943	0.0026801
	PSO-ELM	150	0.0072654	0.99573	0.0062117
	DGWO-ELM	350	0.0005389	0.99974	0.0004148
	PSO-ELM	350	0.1006976	0.99055	0.0077731
Y6	DGWO-ELM	100	0.0054873	0.99805	0.0034437
	PSO-ELM	100	0.0118545	0.98947	0.0109327
	DGWO-ELM	250	0.0001054	0.99999	0.0001067
	PSO-ELM	250	0.0006985	0.99994	0.0007878

and then discuss their results. Figure 7 shows the prediction results of the three algorithms under the Y3 experimental data at the training length of 200, 300, and 400, respectively.

It can be seen from Fig. 7 that the DGWO-ELM algorithm has high predictive accuracy, Moreover, its accuracy is proportional to the number of training cycles. The blue line is closest to the real data, the green line is second, and the worst result is the purple line. The DGWO-ELM algorithm is superior to the other two algorithms in both short and long prediction cycles. The worst predictive algorithm is the GWO-SVM algorithm.

Figure 8 below shows the prediction results of the three algorithms under the experimental data of the Y4, Y5, and Y6 groups at the training length of 400, 400, and 200, respectively.

In order to further validate the effectiveness of the proposed algorithm, the prediction results under Y4, Y5 and Y6 of the three algorithms is compared in this paper. The Y6 data sets is smaller than the other two data sets, so the training cycles of Y6 is set to 200, and the battery training cycles of the other two sets are set to 400. As shown in Figure 8, the blue line and the green line are close to the red line, while the purple line is far. Both the PSO-ELM algorithm and the DGWO-ELM algorithm improve the ELM algorithm, so the ELM algorithm is superior to the SVM algorithm. It can be seen from Figure 7 that the PSO-ELM algorithm is easy to fall into the local optimum in the later stage, which makes the algorithm prediction result worse in the later stage. The DGWO-ELM algorithm has excellent prediction performance throughout the whole stage, which makes it better than the PSO-ELM algorithm and the GWO-SVM.

IV. DISCUSSION

A. EXPERIMENT DISCUSSION

In the table, R(cycle) is the training period. Three evaluation functions which are the mean absolute error (MAE), R^2 ,

TABLE 2. Comparison between DGWO-ELM and other algorithms.

Algorithm	Cell Num.	Start cycle(n)	RMSE
PF-SVR[36]	5	50	1.46%
	6	50	2.48%
	7	50	1.47%
FVS-SVR[37]	5	61	1.11%
	6	53	1.51%
	7	78	0.26%
DGWO-ELM	5	56	1.06%
	6	50	0.97%
	7	70	0.43%

root mean squared error (RMSE) are selected to evaluate prediction results.

From Table 1, we can see the comparison between the PSO-ELM algorithm and the DGWO-ELM algorithm. The DGWO-ELM algorithm can maintain good prediction results in short period under different data sets. As can be seen from the short-period and long-period prediction results under the same data set, the DGWO-ELM algorithm has high stability and strong robustness. In DGWO-ELM algorithm, R^2 value is close to one and has better prediction results than the PSO-ELM in terms of other evaluation indicators.

B. OTHER DISCUSSION

1) CONSTANT-CURRENT DISCHARGE

Table 2 shows experiment results of different algorithms by same data sets. Particle Filter (PF) with Support Vector Regression (PF-SVR), Feature vector selection (FVS) with SVR (FVS-SVR) and DGWO-ELM algorithm share the

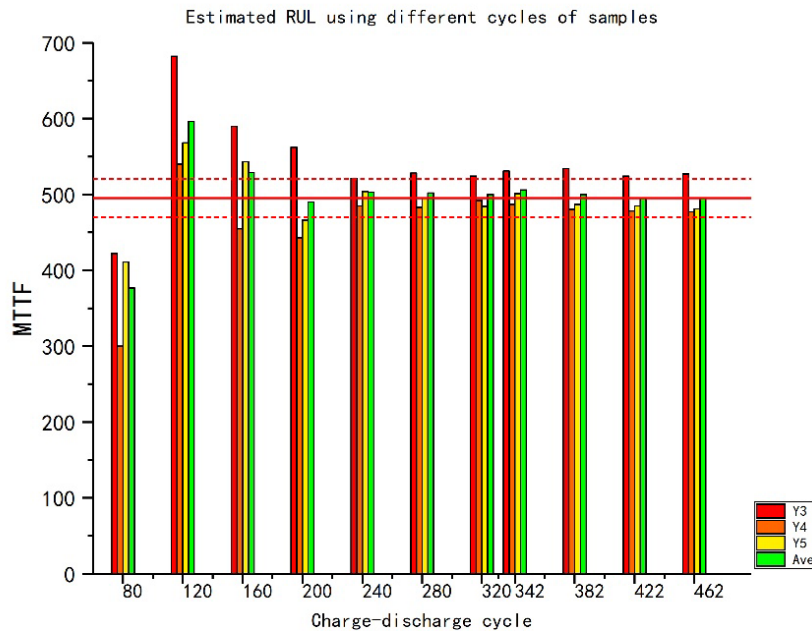


FIGURE 9. MTTFs of the batteries extracted using the DGWO-ELM algorithm.

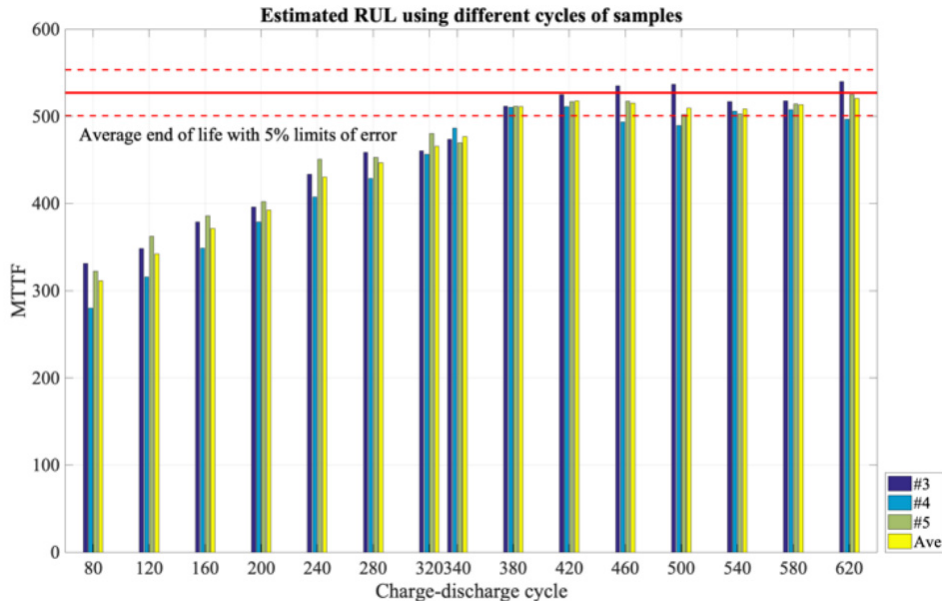


FIGURE 10. MTTFs of the batteries extracted using the gamma process model.

same data set. The RUL threshold of battery is set to 72% nominal capacity. From table 2 we can see that DGWO-ELM is better than PF-SVR algorithm and FVS-SVR algorithm.

2) RANDOM DISCHARGE

The failure threshold of the battery is set to 1.4Ah and the failure point is selected as the first point below 1.4Ah. The end-of-life cycles of data sets Y3, Y4, Y5, and Y6 are 527, 478, 482 and 346, respectively. The experimental data of Y6

is not considered because its degradation mechanism may be different from the other batteries [23]. The average end-of-life cycle of this set of batteries is the average of Y3, Y4, Y5 life cycle, which is 514. Figure 9 is the chart of MTTFs of the batteries extracted using the DGWO-ELM algorithm.

Figure 10 is quoted from the reference 25, where the failure threshold and the average end-of-life cycle are slightly different from their values in this experiment (this experiment linearizes the NASA data and takes the value). The

DGWO-ELM algorithm is data driven and the Gamma Process Model is model driven. Therefore, this experiment only compares which algorithm can achieve reasonable prediction accuracy the fastest in random discharge cycles. From Figure 9 and Figure 10, we can see that the algorithm in reference 25 has good prediction results after 380 cycles, and the DGWO-ELM algorithm has good prediction results after 240 cycles. Compared with the former, the DGWO-ELM algorithm has better predictive results on RUL.

V. CONCLUSION

In this essay, a new algorithm “DGWO-ELM” has been used to predict the battery RUL in the random discharge environment of lithium-ion batteries. The DGWO algorithm is obtained by improving the searching mode, rank and the memory factors of the GWO algorithm. The ELM algorithm is combined with the DGWO algorithm in this essay, in order to improve the input weights and the bias so as to reinforce its prediction accuracy. The DGWO-ELM algorithm was combined with the DE algorithm in this essay to prevent the algorithm from falling into local optimum and then was compared with the GWO-SVM and the PSO-ELM algorithm. In the experimental part, the algorithm was verified from constant current discharge battery dataset by NASA. Then the dataset published by NASA was introduced into the DGWO-ELM to prove that the algorithm can predict the random discharging process of lithium-ion battery. The DGWO-ELM algorithm is proven to be capable to predict the RUL under working conditions. This paper compares the DGWO-ELM algorithm with the algorithms mentioned in other articles to prove the effectiveness of the algorithm.

The amount of sampling points of the NASA random discharge experiment battery capacity data is too small. In the future, we should design such experiments, and set up more sampling points to obtain more usable random battery discharge dataset.

REFERENCES

- [1] L. Chen, L. Xu, and Y. Zhou, “Novel approach for lithium-ion battery on-line remaining useful life prediction based on permutation entropy,” *Energies*, vol. 11, no. 4, p. 820, Apr. 2018.
- [2] H. Zhang, Q. Miao, X. Zhang, and Z. Liu, “An improved unscented particle filter approach for lithium-ion battery remaining useful life prediction,” *Microelectron. Rel.*, vol. 81, pp. 288–298, Feb. 2018.
- [3] F. Guo, G. Hu, S. Xiang, P. Zhou, R. Hong, and N. Xiong, “A multi-scale parameter adaptive method for state of charge and parameter estimation of lithium-ion batteries using dual Kalman filters,” *Energy*, vol. 178, pp. 79–88, Jul. 2019.
- [4] Z. Chen, L. Yang, X. Zhao, Y. Wang, and Z. He, “Online state of charge estimation of Li-ion battery based on an improved unscented Kalman filter approach,” *Appl. Math. Model.*, vol. 70, pp. 532–544, Jun. 2019.
- [5] X. Zheng and H. Fang, “An integrated unscented Kalman filter and relevance vector regression approach for lithium-ion battery remaining useful life and short-term capacity prediction,” *Rel. Eng. Syst. Safety*, vol. 144, pp. 74–82, Dec. 2015.
- [6] J. Luo, J. Peng, and H. He, “Lithium-ion battery SOC estimation study based on cubature Kalman filter,” *Energy Procedia*, vol. 158, pp. 3421–3426, Feb. 2019.
- [7] B. Saha and K. Goebel, “Uncertainty management for diagnostics and prognostics of batteries using Bayesian techniques,” in *Proc. IEEE Aerosp. Conf.*, Mar. 2008, pp. 1–8.
- [8] C. I. Ossai, “Prognosis and remaining useful life estimation of lithium-ion battery with optimal multi-level particle filter and genetic algorithm,” *Batteries*, vol. 4, no. 2, p. 15, Feb. 2018.
- [9] H. S. Ramadan, M. Becherif, and F. Claude, “Extended Kalman filter for accurate state of charge estimation of lithium-based batteries: A comparative analysis,” *Int. J. Hydrogen Energy*, vol. 42, pp. 29033–29046, Sep. 2017.
- [10] Q. Miao, L. Xie, H. Cui, W. Liang, and M. Pecht, “Remaining useful life prediction of lithium-ion battery with unscented particle filter technique,” *Microelectron. Rel.*, vol. 53, pp. 805–810, Jun. 2013.
- [11] S.-L. Wang, C. Fernandez, W. Cao, C.-Y. Zou, C.-M. Yu, and X.-X. Li, “An adaptive working state iterative calculation method of the power battery by using the improved Kalman filtering algorithm and considering the relaxation effect,” *J. Power Sources*, vol. 428, pp. 67–75, Jul. 2019.
- [12] X. Wang, B. Jiang, and N. Lu, “Adaptive relevant vector machine based RUL prediction under uncertain conditions,” *ISA Trans.*, vol. 87, pp. 217–224, Apr. 2019.
- [13] M. A. Patil, P. Tagade, K. S. Hariharan, S. M. Kolake, T. Song, T. Yeo, and S. Doo, “A novel multistage support vector machine based approach for Li ion battery remaining useful life estimation,” *Appl. Energy*, vol. 159, pp. 285–297, Dec. 2015.
- [14] L.-L. Li, Z.-F. Liu, M. L. Tseng, and A. S. F. Chiu, “Enhancing the Lithium-ion battery life predictability using a hybrid method,” *Appl. Soft Comput.*, vol. 74, pp. 110–121, Jan. 2019.
- [15] S. Li, H. He, and J. Li, “Big data driven lithium-ion battery modeling method based on SDAE-ELM algorithm and data pre-processing technology,” *Appl. Energy*, vol. 242, pp. 1259–1273, May 2019.
- [16] J. Yang, Z. Peng, Z. Pei, Y. Guan, H. Yuan, and L. Wu, “Remaining useful life assessment of lithium-ion battery based on HKA-ELM algorithm,” *Int. J. Electrochem. Sci.*, vol. 13, no. 10, pp. 9257–9272, 2018.
- [17] J. Yang, Z. Peng, H. Wang, H. Yuan, and L. Wu, “The remaining useful life estimation of lithium-ion battery based on improved extreme learning machine algorithm,” *Int. J. Electrochem. Sci.*, vol. 13, pp. 4991–5004, May 2018.
- [18] J. Wu, C. Zhang, and Z. Chen, “An online method for lithium-ion battery remaining useful life estimation using importance sampling and neural networks,” *Appl. Energy*, vol. 173, pp. 134–140, Jul. 2016.
- [19] Z. Chen, S. Cao, and Z. Mao, “Remaining useful life estimation of aircraft engines using a modified similarity and supporting vector machine (SVM) approach,” *Energies*, vol. 11, no. 1, p. 28, Jan. 2018.
- [20] F. Tobar, I. Castro, J. Silva, and M. Orchard, “Improving battery voltage prediction in an electric bicycle using altitude measurements and kernel adaptive filters,” *Pattern Recognit. Lett.*, vol. 105, pp. 200–206, Apr. 2018.
- [21] A. Soualhi, K. Medjaher, and N. Zerhouni, “Bearing health monitoring based on Hilbert–Huang transform, support vector machine, and regression,” *IEEE Trans. Instrum. Meas.*, vol. 64, no. 1, pp. 52–62, Jan. 2015.
- [22] D. Wang, F. Yang, Y. Zhao, and K.-L. Tsui, “Battery remaining useful life prediction at different discharge rates,” *Microelectron. Rel.*, vol. 78, pp. 212–219, Nov. 2017.
- [23] Z. Wu, Z. Wang, C. Qian, B. Sun, Y. Ren, Q. Feng, and D. Yang, “Online prognostication of remaining useful life for random discharge lithium-ion batteries using a gamma process model,” in *Proc. 20th Int. Conf. Therm., Mech. Multi-Phys. Simulation Exp. Microelectron. Microsyst.*, Mar. 2019, pp. 1–6.
- [24] A. M. Abdelshafy, H. Hassan, and J. Jurasz, “Optimal design of a grid-connected desalination plant powered by renewable energy resources using a hybrid PSO-GWO approach,” *Energy Convers. Manage.*, vol. 173, pp. 331–347, Oct. 2018.
- [25] P. García-Triviño, F. Llorens-Iborra, C. A. García-Vázquez, A. J. Gil-Mena, L. M. Fernández-Ramírez, and F. Jurado, “Long-term optimization based on PSO of a grid-connected renewable energy/battery/hydrogen hybrid system,” *Int. J. Hydrogen Energy*, vol. 39, pp. 10805–10816, Jul. 2014.
- [26] B. Saha and K. Goebel. (2007). Battery Data Set. NASA AMES Prognostics Data Repository; National Aeronautics and Space Administration (NASA’s) AMES Research Center: Moffett Field, CA, USA. [Online]. Available: <http://ti.arc.nasa.gov/tech/dash/pcoe/prognostic-data-repository/>
- [27] S. Tang, C. Yu, X. Wang, X. Guo, and X. Si, “Remaining useful life prediction of lithium-ion batteries based on the Wiener process with measurement error,” *Energies*, vol. 7, no. 2, pp. 520–547, Jan. 2014.
- [28] T. S. Bryden, A. Holland, G. Hilton, B. Dimitrov, C. P. de León Albarrán, and A. Cruden, “Lithium-ion degradation at varying discharge rates,” *Energy Procedia*, vol. 151, pp. 194–198, Oct. 2018.

- [29] S. Panchal, M. Mathew, R. Fraser, and M. Fowler, "Electrochemical thermal modeling and experimental measurements of 18650 cylindrical lithium-ion battery during discharge cycle for an EV," *Appl. Therm. Eng.*, vol. 135, pp. 123–132, May 2018.
- [30] F. Meng, L. Chen, and Z. Xie, "Numerical simulations and analyses on thermal characteristics of 18650 lithium-ion batteries with natural cooling conditions," *Energy Environ.*, vol. 8, no. 1, pp. 43–50, 2017.
- [31] F. Feng, R. Lu, and C. Zhu, "A combined state of charge estimation method for lithium-ion batteries used in a wide ambient temperature range," *Energies*, vol. 7, no. 5, pp. 3004–3032, May 2014.
- [32] Y. Zhang, R. Xiong, H. He, and M. G. Pecht, "Lithium-ion battery remaining useful life prediction with box-cox transformation and Monte Carlo simulation," *IEEE Trans. Ind. Electron.*, vol. 66, no. 2, pp. 1585–1597, Feb. 2019.
- [33] S. Liu, J. Wang, Q. Liu, J. Tang, H. Liu, and Z. Fang, "Deep-discharging li-ion battery state of charge estimation using a partial adaptive forgetting factors least square method," *IEEE Access*, vol. 7, pp. 47339–47352, 2019.
- [34] K. Amine, J. Liu, and I. Belharouak, "High-temperature storage and cycling of C-LiFePO₄/graphite Li-ion cells," *Electrochem. Commun.*, vol. 7, pp. 669–673, Jul. 2005.
- [35] M. S. H. Lipu, M. A. Hannan, A. Hussain, M. M. Hoque, P. J. Ker, M. H. M. Saad, and A. Ayob, "A review of state of health and remaining useful life estimation methods for lithium-ion battery in electric vehicles: Challenges and recommendations," *J. Cleaner Prod.*, vol. 205, pp. 115–133, Dec. 2018.
- [36] J. Wei, G. Dong, and Z. Chen, "Remaining useful life prediction and state of health diagnosis for lithium-ion batteries using particle filter and support vector regression," *IEEE Trans. Ind. Electron.*, vol. 65, no. 7, pp. 5634–5643, Jul. 2018.
- [37] Q. Zhao, X. Qin, H. Zhao, and W. Feng, "A novel prediction method based on the support vector regression for the remaining useful life of lithium-ion batteries," *Microelectron. Rel.*, vol. 85, pp. 99–108, Jun. 2018.
- [38] S. Zhao, Y. Zhang, S. Wang, B. Zhou, and C. Cheng, "A recurrent neural network approach for remaining useful life prediction utilizing a novel trend features construction method," *Measurement*, vol. 146, pp. 279–288, Nov. 2019.
- [39] G. Ma, Y. Zhang, C. Cheng, B. Zhou, P. Hu, and Y. Yuan, "Remaining useful life prediction of lithium-ion batteries based on false nearest neighbors and a hybrid neural network," *Appl. Energy*, vol. 253, Nov. 2019, Art. no. 113626. doi: [10.1016/j.apenergy.2019.113626](https://doi.org/10.1016/j.apenergy.2019.113626).



JUN ZHU was born in Beijing, China, in 1994. He is currently pursuing the master's degree with the School of Information Engineering, Capital Normal University of China. His research interests include health management and prediction of lithium batteries and fault diagnosis of electronic system.



TIANXIONG TAN was born in Beijing, China, in 1995. He is currently pursuing the master's degree with the School of Information Engineering, Capital Normal University of China. His research interests include data-driven modeling and electrical vehicles.



LIFENG WU (M'12) received the B.S. degree in applied physics from the China University of Mining and Technology, in 2002, the M.S. degree in detection technology and automation device from Northeast Electric Power University, in 2005, and the Ph.D. degree in physical electronics from the Beijing University of Posts and Telecommunications, in 2010. From 2012 to 2013, he was a Visiting Scholar with Tsinghua University. From 2014 to 2015, he was a Postdoctoral with the University of Maryland, College Park, USA. From 2017 to 2018, he was a Visiting Scholar with Peking University. He is currently a Professor with Capital Normal University. His research interests include data-driven modeling, estimation and filtering, fault diagnosis, power electronics, and electrical vehicles.



HUIMEI YUAN (M'12) received the Ph.D. degree in electrical automation from the China Agricultural University, in 1999. From 2004 to 2008, she was a Postdoctoral with the College of Automation, University of Beihang, China. Since 2010, she has been a Professor with Capital Normal University. Her research interests include signal processing, fault diagnosis, power electronics, and electrical vehicles.